SUB-TRIANGLE SHOOTING RAY-TRACING IN COMPLEX 3D VTI MEDIA

TAO XU[1], ZHONGJIE ZHANG[1], AIHUA ZHAO[2], ANJIA ZHANG[1], XI ZHANG[1] and HONGSHUANG ZHANG[1]

[1] *State Key Laboratory of Lithosphere Evolution, Institute of Geology and Geophysics, Chinese Academy of Sciences, China.*
[2] *Institute of Geology and Geophysics, China Earthquake Administration, China.*
xutao@mail.iggcas.ac.cn

(Received October, 2006; revised version accepted October 10, 2007)

ABSTRACT

Xu, T., Zhang, Z., Zhao, A., Zhang, A., Zhang, X. and Zhang, H., 2008. Sub-triangle shooting ray-tracing in complex 3D VTI media. In: Liu, E., Zhang, Z.-J. and Li, X.-Y. (Eds.), Seismic Anisotropy. *Journal of Seismic Exploration*, 17: 133-146.

We model a complex 3D anisotropic structure as an aggregate of arbitrarily shaped blocks or volumes separated by triangulated interfaces, and different anisotropic parameters can be defined in different blocks. In anisotropic media, seismic wave travels in the direction of ray vectors with group velocities throughout a ray trajectory, therefore, group velocities expressed by ray angles is required, but difficult to express in terms of phase angles. An approximate expression in terms of ray angles is derived for weak transversely isotropic media with a vertical symmetry axis (VTI). We also propose a simple iterative process to calculate ray angles in terms of the Snell's law still valid for phase velocities and phase angles. Modification of shooting angles is crucial in implementing 3D shooting ray-tracing, and we suggest to use the sub-triangle shooting method to update the shooting angles to enhance the computing efficiency. Numerical tests demonstrate that a blocky model can be a good description of complex 3D VTI media and the sub-triangle shooting ray-tracing is very effective to implement for kinematics two-point ray-tracing.

KEY WORDS: phase velocity, group velocity, Snell's law, ray-tracing.

0963-0651/08/$5.00

INTRODUCTION

Recently, many researchers have focused on developing ray-tracing techniques in anisotropic media (Vinje et al., 1996; Slawinski et al., 2000; Kumar et al., 2004; Pšenčík and Farra, 2005; Zhao et al., 2006). For ray-tracing in anisotropic media, three key issues should be considered: (1) ray vectors and phase vectors are not coincident; group velocities expressed by ray (group) angles are convenient but difficult to obtain. Some approximate expressions have been published for weak anisotropy (Byun et al., 1989; Sena, 1991). In this paper we propose alternative approximation to enhance the efficiency of computations. (2) Snell's law is only valid for phase velocities and phase angles, but is invalid for group velocities and ray angles (Slawinski et al., 2000). The calculation of ray angles for reflected and refracted rays from incidence ray angles is a nonlinear problem. We propose a simply iterative method to calculate ray angles for reflected and refracted rays. (3) In most applications, the parameterization of anisotropic models are often grid-based and for stratified layers (Sena, 1991; Slawinski et al., 2000; Kumar et al., 2004; Zhao et al., 2006). A fine grid-based model is a good approximation, but often computationally extensive. We need to describe in general complex 3D models for practical applications (Xu et al., 2006). We extend the blocky models to describe anisotropic media and implement a sub-triangle ray-tracing method in VTI media.

TRANSVERSELY ISOTROPIC BLOCKY MODELS

Most ray-tracing methods are based on models parameterized in cells or grids (Langan et al., 1985; Moser, 1991; Soukina et al., 2003) or layers (Zelt and Smith, 1992; Gui Ziou et al., 1996; Rawlinson et al., 2001). When we divide a model into fine enough cells or grids if the model is complex with large lateral and vertical variations. The computation time of the algorithms is almost linearly proportional to the number of nodes in the models when traveltimes need to be computed for all nodes (Moser, 1991); therefore, ray-tracing can be very time-consuming for these models, especially in 3D. To overcome the difficulty mentioned above, a 3D complex model can be thought as an aggregate of arbitrarily shaped blocks or volumes separated by triangulated interfaces (Xu et al., 2006). The structures are regarded hierarchically as volumes → blocks → interfaces → triangles → points. Geological blocks are separated by interfaces, which are described by several discrete points and are triangulated. One of the advantages of triangulated interface as opposed to Coons, Bezier and B-spline surface patches is that discrete points do not need to be defined in a rectangular domain. Modification and elimination of accurate geological nodes are also easy to implement. Furthermore, the intersection between a line and a triangle can be computed analytically and hence the large number of ray/interface intersections can be computed quickly.

The disadvantages of triangulated interfaces include that they are less smooth, normal vectors vary abruptly across linked boundary of two triangles that are not in the same plane, and sometimes it is difficult to find an optimal solution. These can be partly solved by redefining normal vectors at arbitrary points so that normal vectors are continuous on the whole interfaces. The advantages and disadvantages of blocky models with triangulated interfaces have been summarized by Xu et al. (2006). Here, we extend our previous work on isotropic ray-tracing to anisotropic media and describe different anisotropic group velocities in different blocks.

GROUP VELOCITY AND RAY ANGLES IN VTI MEDIA

Daley and Hron (1977) gave phase velocities of qP-, qSV- and qSH-waves in terms of phase angles

$$\rho v_p^2(\theta) = \tfrac{1}{2}[C_{33} + C_{44} + (C_{11} - C_{33})\sin^2\theta + D(\theta)] \quad , \tag{1}$$

$$\rho v_{sv}^2(\theta) = \tfrac{1}{2}[C_{33} + C_{44} + (C_{11} - C_{33})\sin^2\theta - D(\theta)] \quad , \tag{2}$$

$$\rho v_{SH}^2(\theta) = C_{66}\sin^2\theta + C_{44}\cos^2\theta \quad , \tag{3}$$

$$\begin{aligned} D^2(\theta) = {} & (C_{33} - C_{44})^2 + 2[2(C_{13} + C_{44})^2 \\ & - (C_{33} - C_{44})(C_{11} + C_{33} - 2C_{44})]\sin^2\theta \\ & + [(C_{11} + C_{33} - 2C_{44})^2 - 4(C_{13} + C_{44})^2]\sin^2\theta \quad , \end{aligned} \tag{4}$$

where ρ is the density, and C_{ij} (i,j = 1, 2, ..., 6) are elastic moduli. The phase angle θ is the angle between the wavefront normal and the vertical axis of the symmetry plane. Ray angle ϕ is the angle from the source point to the wavefront. The relationship between ray angle ϕ and phase angle θ is given below:

$$\phi = \theta + f(\theta) \quad , \tag{5}$$

where

$$f(\theta) = \arctan[(1/v)(dv/d\theta)] \quad . \tag{6}$$

For three body waves, we have

$$\begin{aligned} f_P(\theta) = {} & \arctan\{[(C_{11} - C_{33})\sin\theta\cos\theta + D^*(\theta)] \\ & /[C_{33} + C_{44} + (C_{11} - C_{33})\sin^2\theta + D(\theta)]\} \quad , \end{aligned} \tag{7}$$

$$f_{SV}(\theta) = \arctan\{[(C_{11} - C_{33})\sin\theta\cos\theta - D^*(\theta)] / [C_{33} + C_{44} + (C_{11} - C_{33})\sin^2\theta - D(\theta)]\} \quad , \tag{8}$$

$$f_{SH}(\theta) = \arctan\{[(C_{66} - C_{44})\sin\theta\cos\theta - D^*(\theta)] / [C_{66}\sin^2\theta + C_{44}\cos^2\theta]\} \quad , \tag{9}$$

$$D^*(\theta) = [1/D(\theta)] \{[2(C_{13} + C_{44})^2 - (C_{33} - C_{44})(C_{11} + C_{33} - 2C_{44})]\sin\theta\cos\theta + [(C_{11} + C_{33} - 2C_{44})^2 - 4(C_{13} + C_{44})^2]\sin^3\theta\cos\theta\} \quad . \tag{10}$$

The group velocity can be obtained from phase velocity and phase angle as below:

$$V(\phi) = v^2(\theta) + (dv/d\theta)^2 = v(\theta)\sec f(\theta) \quad . \tag{11}$$

In anisotropic media, seismic waves travel in the direction along the ray vector with group velocities throughout a ray trajectory. Therefore, group velocities expressed by ray angles is required in ray-tracing. In weak anisotropic media, some approximations of group velocities in terms of ray angles are presented by using a linear approximation (Sena, 1991) and a cosine polynomial function (Byun, 1989).

In weak anisotropic media, the ray angle is close to the corresponding phase angle. We propose the following expression

$$\theta = \phi - \tfrac{1}{2}[f(\phi) + f(\phi - f(\phi))] \quad . \tag{12}$$

For a given ray angle ϕ, we can obtain a corresponding approximate phase angle θ using eq. (12), and then we can calculate the group velocity using eq. (11).

Numerical calculation proves that this approximation is more accurate than the linear approximation (Sena, 1991) and is similar to the cosine polynomial function (Byun, 1989), and even more accurate for qSV waves (Zhao and Ding, 2005; Zhao et al., 2006).

REFLECTION AND TRANSMISSION

Slawinski et al. (2000) extended Snell's law in terms of slowness surfaces in anisotropic media. As phase velocities are functions of phase angles in

anisotropic media, given an incidence phase angle, phase angles for reflected and refracted rays can be obtained by solving a quadratic equation (Slawinski et al., 2000).

Here we propose a simple iterative method to compute ray angles for reflected and refracted rays at arbitrary points on an interface. The procedure includes three steps:

a. use eqs. (12) and (1), (2), (3) to calculate the incident phase angle and phase velocities from a given incidence ray angle and the corresponding group velocities;

b. calculate phase angles using Snell's law;

c. use eqs. (5) and (11) to calculate the ray angles for reflected and refracted rays and group velocities.

In step (b), we calculate the phase angle θ_2 and phase velocity v_2 using

$$\sin\theta_1 / v_1(\theta_1) = \sin\theta_2 / v_2(\theta_2) \quad . \tag{13}$$

where θ_1 is the given phase angle and v_1 is the corresponding phase velocity. As $v_2(\theta_2)$ is the nonlinear function of θ_2 [eqs. (1)-(3)], here we propose a simple iterative method:

a. given an initial phase angle θ_2;

b. calculate the phase velocity v_2 in the direction of θ_2;

c. using Snell's law [eq. (13)], new phase angles θ_2' for the reflected and refracted rays can be calculated;

d. if the difference between θ_2' and θ_2 is smaller than a given threshold, the process stops; otherwise, define $\theta_2 = \theta_2'$, go back to the first step.

Our iterative process is similar to that proposed by Slawinski et al. (2000). The main difference is that we calculate ray angles from reflected and refracted phase angles by an iteration procedure, while Slawinski et al. (2000) propose to solve a quadratic equation.

Numerical tests indicate that the phase angle converges very quickly in the iteration process. In weakly anisotropic media, the choice of the initial phase angle has very little influence in the velocity convergence. If given the initial phase θ_2 equals to θ_1, the phase angle will converge to a given precision (typically 1% error) after two or three iterations.

SUB-TRIANGLE SHOOTING METHOD

Xu et al. (2006) have presented a segmentally iterative ray-tracing method for complex 3D blocky models. However, the method cannot be directly applied to anisotropic media, as their iterative formulations have not considered velocities variation with shooting angles. Here we propose a sub-triangle shooting method, which is robust in handling ray-tracing in complex 3D anisotropic media.

Modification of shooting angles is the key to perform 3D ray-tracing, which affects whether shooting angles can converge quickly. We introduce the shooting ray-tracing method using 3D reflected waves as an object. Firstly, a bunch of rays are shot at an angle range in both vertical and horizontal planes and hence generating a matrix of shot angles. These shooting rays produce the mesh emergence points on the surface, as shown in Fig. 1. These mesh points form a set of triangles, called emergence triangles. The three vertexes of emergence triangles correspond to shooting angles (θ_i,ϕ_i) as well as direction components $(\sin\theta_i\cos\phi_i,\sin\theta_i\sin\phi_i,\cos\theta_i)$, denoted by w_i, where $i = 1,2,3$. With the aid of area coordinates (Xu et al., 2004, 2006), it can easily and rapidly determine the triangle where a target receiver P is situated. When the positions of receivers, three vertexes of the situated triangles, and the corresponding shooting angles (or direction components) are known, the shooting ray-tracing is a process to update shooting angles so that the rays are directed towards the receivers. As it is a nonlinear problem, the iteration is required.

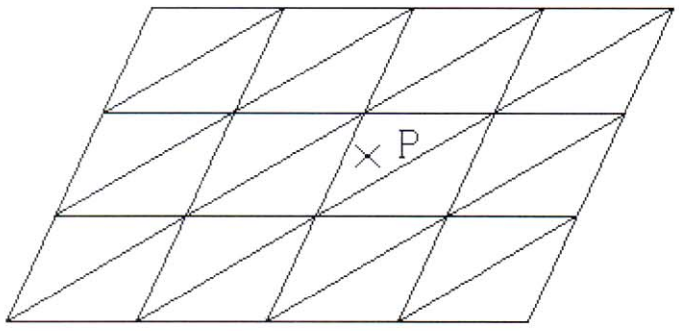

Fig. 1. The emergence points form a set of so-called emergence triangles (Cross P is a receiver)

As shown in Fig. 2, the receiver P lies inside the emergence triangle $T_1T_2T_3$. Suppose that the shooting direction components of three vertexes are $w_j^{(i)}$, where (i,j = 1,2,3), i denotes the sequence number and j represents three components. Let the area coordinates of the receiver P in the triangle be u_i, the new component w_j in the shooting direction is then given by

$$w_j = \sum_{i=0}^{3} w_j^{(i)} u_i \quad . \tag{14}$$

We perform shooting in this new direction and hence obtain the emergence point T_4. If the distance between T_4 and the receiver is less than a given precision, the shooting iteration stops. Otherwise we construct an equilateral triangle $T_4T_5T_6$, where the emergence point T_4 is one vertex and the receiver P is at the centre. Using shooting direction components of three vertexes T_1, T_2, T_3, and performing weighted summation over area coordinates of T_5 and T_6 in the triangle, new direction components are calculated as eq. (14) for the next shooting to generate another two emergence points T_5' and T_6'. Because of nonlinearity, there is no coincidence between T_5' and T_5, T_6' and T_6. The shooting emergence points T_4, T_5' and T_6' constitute a new initial triangle for the shooting iteration. Continuing the procedures above for the shooting iteration until the distance between the new emergence point and the receiver is less than a given precision.

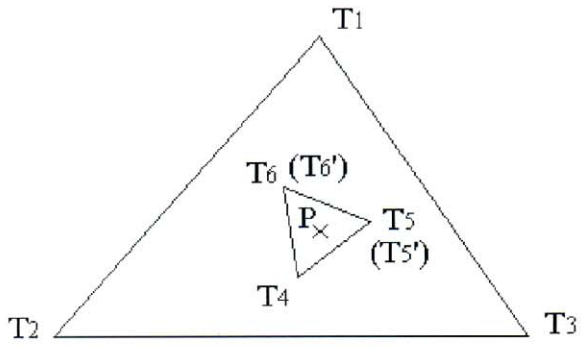

Fig. 2. The sketch map of the sub-triangle method to update shooting angles.

SYNTHETIC DATA EXAMPLES

We present two typical VTI blocky models (Figs. 3 and 5) to illustrate the sub-triangle ray-tracing method. These models, contained within cubes consist of several blocks separated by triangulated interfaces. Both models have dimensions of 5000 × 5000 × 5000 m. X-, Y- and Z-axes are denoted as red, green and blue colour. Fig. 3 (Model 1) shows a simple blocky model with three dipping plane interfaces. Model 1 has 4 blocks (denoted by Roman letters), 3423 triangles and 1626 points. Fig. 5 (Model 2) shows a complex model, composed of normal faults, reverse faults, an intrusive body and a lens, has 7 blocks (denoted by Roman letters) and 4649 triangles and 2152 points. VTI parameters of two models are listed in Tables 1 and 2. Note that $\sqrt{(C_{11}/\rho)}$ and $\sqrt{(C_{33}/\rho)}$ are horizontal and vertical qP-wave phase velocities, and $\sqrt{(C_{44}/\rho)}$ and $\sqrt{(C_{66}/\rho)}$ are vertical and horizontal qSH-wave phase velocities, respectively.

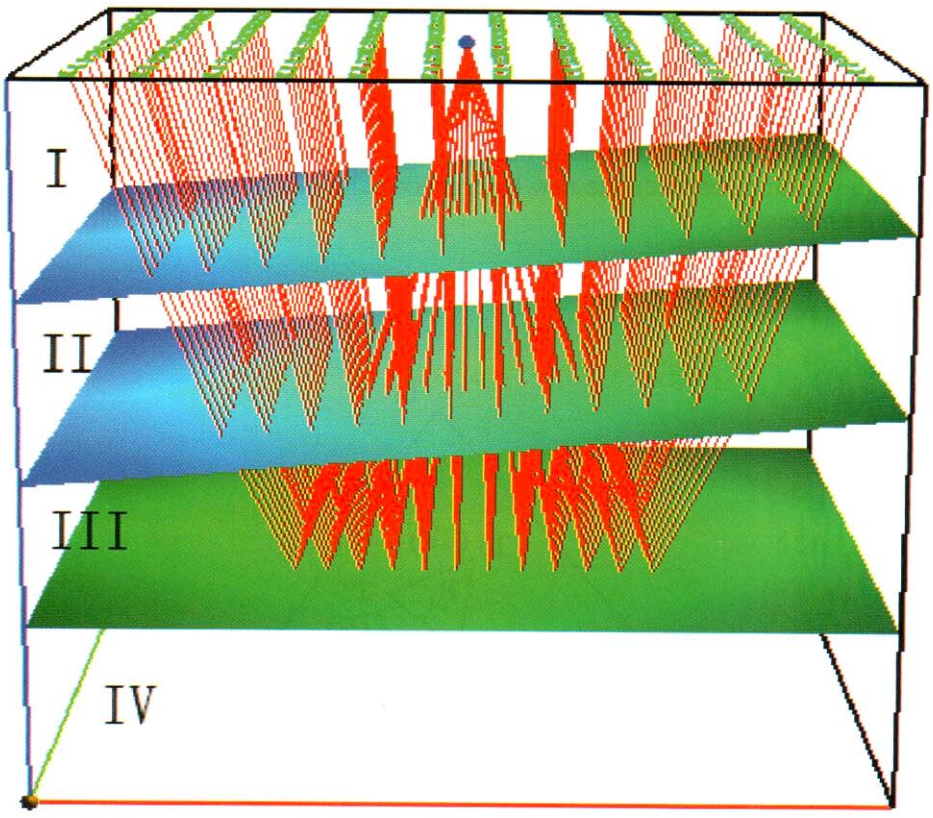

Fig. 3. Model 1 has four blocks (denoted as Roman letters) and 3423 triangles, and corresponding ray-tracing results.

The source-receiver pairs are located on the surface and the locations of the sources and receivers are indicated by stars and triangles, respectively. The third dip layer in Model 1 and the upper interface of the lens in Model 2 are defined as reflecting interfaces. As the distinction of ray trajectories is of a minor symmetry and not intuitive as opposed to traveltime contours, we just show two-point ray-tracing results both in VTI media. Fig. 3 denotes qP-waves in Model 1 and Fig. 5 denotes qSV-waves in Model 2.

Table 1. VTI parameters used in Model 1 (Fig. 3).

Blocks	$\sqrt{(C_{11}/\rho)}$	$\sqrt{(C_{33}/\rho)}$	$\sqrt{(C_{13}/\rho)}$	$\sqrt{(C_{44}/\rho)}$	$\sqrt{(C_{66}/\rho)}$
I	2100	2000	1158	89	880
II	2262	2200	1600	1020	1080
III	2980	2700	2196	1200	1336
IV	3389	3200	2130	1650	2089

Fig. 4 illustrates associated traveltime contours of qP-, qSV- and qSH-waves in Model 1, respectively. Fig. 6 illustrates associated traveltime contours of three waves in Model 2. Solid lines denote traveltime contours in VTI media and dashed lines in homogenous media. Homogenous velocities in each bock are defined as the phase velocities (Table 1). Traveltime contours in homogenous media (dashed lines in Figs. 4a - 4c) are all concentric circles for the three flat interfaces and only tilted in the x-axis direction. Note that traveltime contours in VTI media of three waves show considerable differences. Traveltime contours of qP-waves are closest to those in homogenous media (solid lines in Figs. 4a and 6a) as opposed to the other two waves. As phase velocities are smaller than corresponding group velocities media in VTI media, the traveltimes are smaller and hence traveltime contours are closer to the centre of the circle (Fig. 4a) or closer to the centre (Fig. 6a). For qSH-waves, traveltime contours in VTI media have an offset opposite to those in homogenous media. Traveltime contours have an offset in the positive direction along x-axis when flat interfaces tilted to the negative direction along the x-axis (solid lines in Fig. 4c) and have an opposite offset (solid lines in Fig. 6c) for the reflected interface near the reflected points tilted to the negative direction (along the x-axis positive). There is a distinctive characteristic in traveltime contours for qSV-waves (solid lines in Figs. 4b and 6b) induced by anisotropy. Note that due to the complexity of Model 2, several receivers can not be traced (Fig. 5), as a result, traveltimes contours have major errors in the corresponding position (the left part in Figs. 4 and 6).

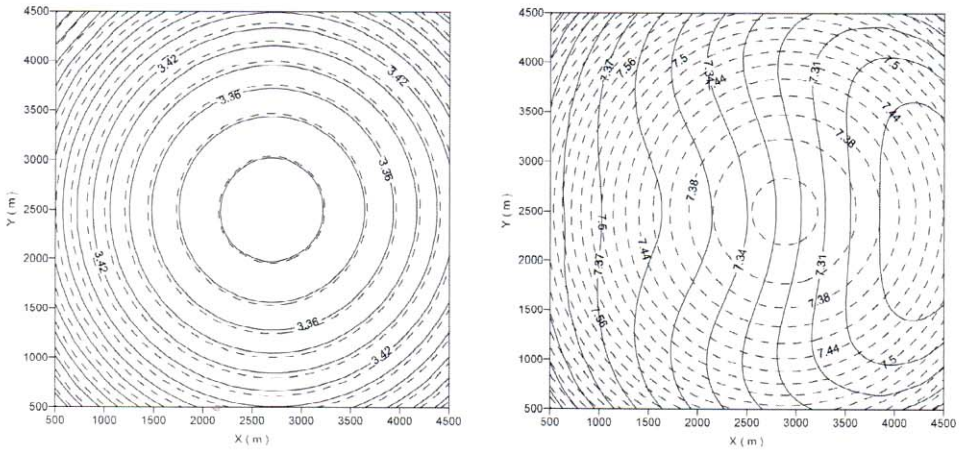

(a) (b)

(c)

Fig. 4. Traveltime contours of three waves ray traced in Model 1 (Fig. 3); solid lines denote in VTI media and dashed lines are for in homogenous media. (a) qP-waves; (b) qSV-waves; (c) qSH-waves.

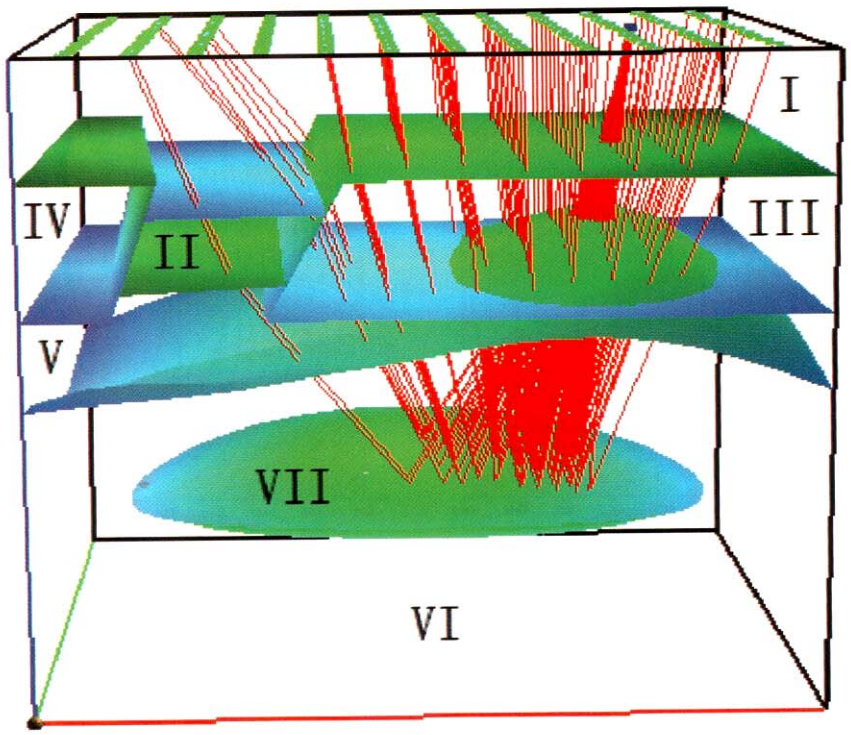

Fig. 5. Model 2, composed of normal faults, reverse faults, an intrusive mass, and a lens, has 7 blocks (denoted as Roman letters) and 4649 triangles, and the corresponding ray-tracing results.

Table 2. VTI parameters used in Model 2 (Fig. 5).

Blocks	$\sqrt{(C_{11}/\rho)}$	$\sqrt{(C_{33}/\rho)}$	$\sqrt{(C_{13}/\rho)}$	$\sqrt{(C_{44}/\rho)}$	$\sqrt{(C_{66}/\rho)}$
I	2000	2000	1158	880	880
II	2262	2200	1600	1020	1080
III	2583	2408	1513	1321	1566
IV	2980	2700	2196	1200	1336
V	3389	3200	2130	1650	2089
VI	3742	3306	2070	1818	2285
VII	5320	4726	2460	2860	3321

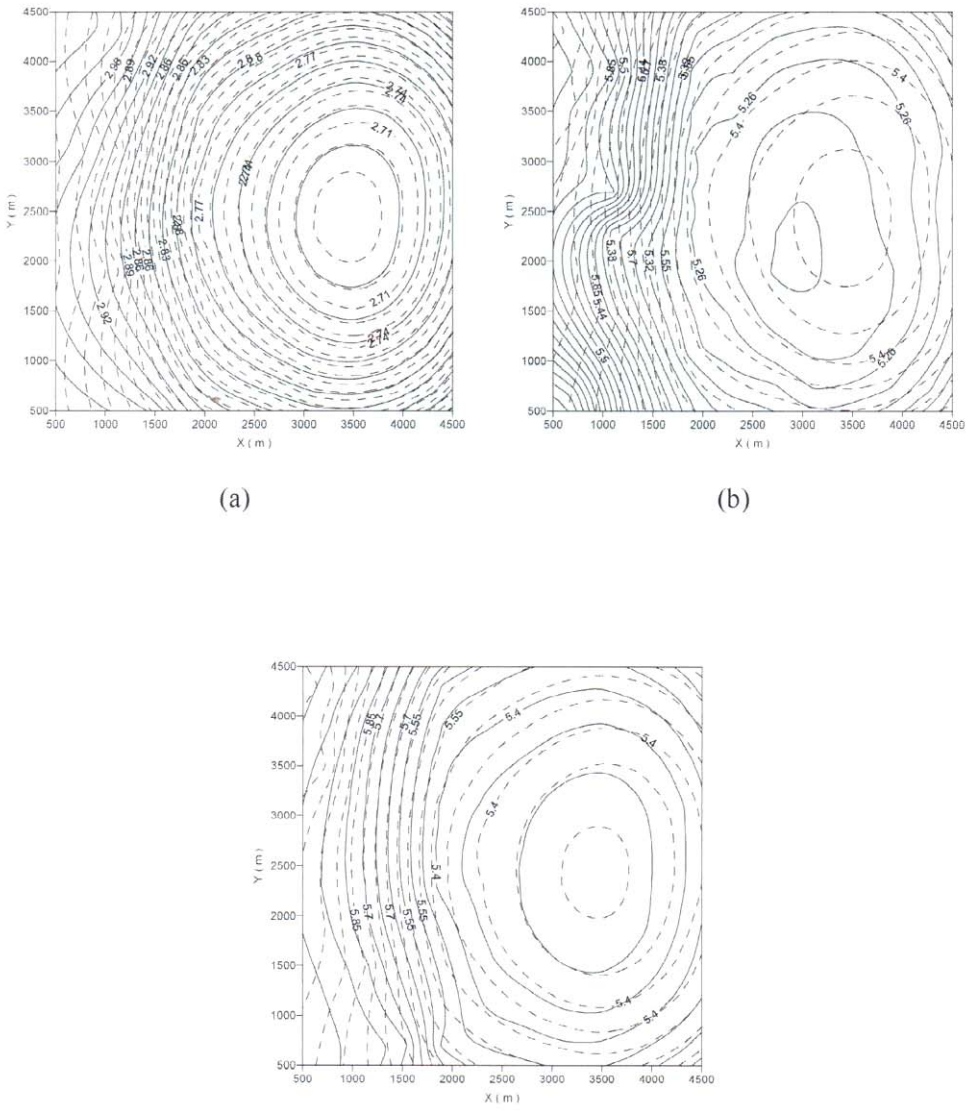

Fig. 6. Traveltime contours of three waves ray traced in Model 2 (Fig. 5); solid lines denote in VTI media and dashed lines are for homogenous media. (a) qP-waves; (b) qSV-waves; (c) qSH-waves.

CONCLUSIONS

Complex anisotropic media can be described accurately as aggregates of arbitrarily shaped blocks than layers, cells or grids. Using triangulated interfaces, complex media, such as faults, pinch-outs, intrusive bodies, and lenses can be realistically represented by blocks. Different anisotropic parameters including group velocities can be defined in different blocks.

As Snell's law is invalid for group velocities and ray angles in anisotropic media, we have proposed a simple iterative procedure to calculate ray angles for reflected and refracted rays. Our approximate expression of group velocities by phase angles is accurate in weak VTI media. The accuracy is similar to the cosine polynomial of Byun et al. (1989), and even more accurate for qSV waves.

We have also extended our previous sub-triangle shooting method in isotropic media to VTI media. Numerical tests demonstrate that a blocky model can be a good description of a complex 3D anisotropic medium and the sub-triangle shooting ray-tracing is effective in implementing kinematics two-point ray-tracing, and our method is quite accurate for ray-tracing in VTI media.

ACKNOWLEDGEMENT

This work was jointly supported by the National 973 Programme China (2002CB412604), and the National Natural Science Foundation of China (grant numbers 40234044, 40374010, 40404009 and 40721003) and the CAS grant kzcx2-yw-132.

REFERENCES

Byun, B.S., Corrigan, D. and Gaiser, J., 1989. Anisotropic velocity analysis for lithology discrimination. Geophysics, 54: 1564-1574.

Daley, P.F. and Hron, F., 1977. Reflection and transmission coefficients for transversely isotropic media. Bull. Seism. Soc. Am., 67: 661-675.

GuiZiou, J.L., Mallet, J. and Madariaga, R., 1996. 3D seismic reflection tomography on top of the GOCAD depth modeler. Geophysics, 61: 1499-1510.

Iversen, E., 2006. Velocity rays for heterogeneous anisotropic media: Theory and implementation. Geophysics, 71: T117-T127.

Kumar, D., Sen, M.K. and Ferguson, R.J., 2004. Traveltime calculation and prestack depth migration in tilted transversely isotropic media. Geophysics, 69: 37-44.

Langan, R.T., Lerche, I. and Cutler, R.L., 1985. Tracing of rays through heterogeneous media, an accurate and efficient procedure. Geophysics, 50: 1456-1465.

Moser, T.J., 1991. Shortest path calculation of seismic rays. Geophysics, 56: 59-67.

Pereyra, V., 1992. Two-point ray-tracing in general 3D media. Geophys. Prosp., 40: 267-287.

Pšenčík, I. and Farra, V., 2005. First-order ray-tracing for qP waves in inhomogeneous, weakly anisotropic media. Geophysics, 70: D65-D75.

Rawlinson, N., Houseman, G.A. and Collins, C.D.N., 2001. Inversion of seismic refraction and wide-angle reflection traveltimes for three dimensional layered crustal structure. Geophys. J. Int, 145: 381-400.

Sena, A.G., 1991. Seismic traveltime equations for azimuthally anisotropic and isotropic media, estimation of interval elastic properties. Geophysics, 56: 2090-2101.

Slawinski, M.A., Slawinski, R.A., Brown, R.J. and Parkin, J.M., 2000. A generalized form of Snell's law in anisotropic media. Geophysics, 65: 632-637.

Soukina, S.M., Gajewski, D. and Kashtan, B.M., 2003. Traveltime computation for 3D anisotropic media by a finite-difference perturbation method. Geophys. Prosp., 51: 431-441.

Sun, Y., 1993. Ray-tracing in 3D media by parameterized shooting. Geophys. J. Int., 114: 145-155.

Thurber, C. and Ellsworth, W., 1980. Rapid solution of ray-tracing problems in heterogeneous media. Bull. Seism. Soc. Am., 70: 1137-1148.

Um, J. and Thurber, C., 1987. A fast algorithm for two-point seismic ray-tracing. Bull. Seism. Soc. Am., 77: 972-986.

Vinje, V., Iverson, E., Åstebol, K. and Gjøystdal, H., 1996. Estimation of multivalued arrivals in 3D models using wavefront construction - Part 1. Geophys. Prosp., 44: 819-842.

Xu, T., Xu, G. and Gao, E., 2004. Block modeling and shooting ray-tracing in complex 3D media. Chin. J. Geophys., 47: 1118-1126.

Xu, T., Xu, G., Gao, E., Jiang, X. and Luo, K., 2005. 3D shooting ray-tracing sub-triangle method. Oil Geophys. Prosp., 40: 391-399

Xu, T., Xu, G., Gao, E., Li, Y., Jiang, X. and Luo, K., 2006. Block modeling and segmentally iterative ray-tracing in complex 3D media. Geophysics, 71: T41-T51.

Zelt, C.A. and Smith, R.B., 1992. Seismic traveltime inversion for 2-D crustal velocity structure. Geophys. J. Int., 108: 16-34.

Zhao, A.H. and Ding, Z.F., 2005. New approximate expressions of Seismic group velocities for weakly anisotropic media. Progr. Geophys., 20: 916-919.

Zhao, A.H., Zhang, M.G. and Ding, Z.F., 2006. Seismic traveltime computation for transversely isotropic media. Chin. J. Geophys., 49: 1762-1769.